Journal of Hazardous Materials 196 (2011) 248–254

Contents lists available at SciVerse ScienceDirect

Journal of Hazardous Materials

journal homepage: www.elsevier.com/locate/jhazmat

The influence of preparation method, nitrogen source, and post-treatment on the photocatalytic activity and stability of N-doped TiO_2 nanopowder

Shaozheng Hu*, Fayun Li, Zhiping Fan

Institute of Eco-environmental Sciences, Liaoning Shihua University, Fushun 113001, PR China

ARTICLE INFO

Article history:
Received 19 May 2011
Received in revised form 6 September 2011
Accepted 6 September 2011
Available online 10 September 2011

Keywords:
Lattice-nitrogen
TiO_2
Photocatalysis
Stability
Post-treatment

ABSTRACT

NH_3 plasma, N_2 plasma, and annealing in flowing NH_3 were used to prepare N doped TiO_2, respectively. XRD, UV–vis spectroscopy, N_2 adsorption, FT-IR, Zeta-potential measurement, and XP spectra were used to characterize the prepared TiO_2 samples. The nitridation procedure did not change the phase composition and particle sizes of TiO_2 samples, but extended its absorption edges to the visible light region. The photocatalytic activities were tested in the degradation of an aqueous solution of a reactive dyestuff, methylene blue, under visible light. The photocatalytic activity and stability of TiO_2 prepared by NH_3 plasma were much higher than that of samples prepared by other nitridation procedures. The visible light activity of the prepared N doped TiO_2 was improved by increasing the lattice-nitrogen content and decreasing adsorbed NH_3 on catalyst surface. The lattice-nitrogen stability of N-doped TiO_2 samples improved after HCl solution washing. The possible mechanism for the photocatalysis was proposed.

1. Introduction

Nanocrystalline TiO_2 has great potential for many applications such as photocatalysis, solar energy conversion, and gas sensor [1,2]. However, with a wide band gap energy of 3.0–3.2 eV, TiO_2 cannot be activated to generate photoexcited electrons and holes to promote redox reaction unless it is irradiated by ultraviolet. This hinders the application of TiO_2 as a photocatalyst with response to solar light or even indoor light. Therefore, it is highly desirable to shift the absorption edge of TiO_2 to the visible light region.

In 2001, Asahi et al. [3] prepared nitrogen doped TiO_2 films by sputtering TiO_2 in a N_2/Ar gas mixture, and concluded that the doped N atoms narrowed the band gap of TiO_2 by mixing N 2p and O 2p states, therefore demonstrating the activity for the decomposition of acetone and methylene blue. Since then, N-doping has become a hot topic and been widely investigated. Heating TiO_2 powders in N_2 and/or NH_3 at elevated temperatures is the conventional method to prepare nitrogen-doped TiO_2 [3]. Besides the energy waste, the treatment at such high temperature usually results in the low surface area due to grain growth, which would decrease the number of photoactive sites. Therefore, new strategies for preparing nitrogen-doped TiO_2, such as sputtering [4], sol–gel [5], ion implantation [6], pulsed laser deposition [7], hydrothermal synthesis [8], and plasma treatment [9] have been proposed more recently.

Non-thermal plasma is composed of atoms, ions and electrons, which are much more reactive than their molecule precursors. Plasma is able to initiate a lot of reactions, which take place efficiently only at elevated temperatures and high pressures, under mild conditions. So far, some literatures on preparation of N doped TiO_2 by plasma treatment have been reported [9–13]. Yamada et al. [9–11] investigated the photocatalytic activity of TiO_2 thin films prepared by plasma treatment using N_2 as nitrogen source. They suggested that the substitutional N-doping contributed to the band gap narrowing, therefore absorbing visible light and demonstrating the photocatalytic activity. Abe et al. [12] prepared N doped TiO_2 by NH_3(10%)/Ar plasma. The influence of the NH_3/Ar gas pressures (50, 300 and 1000 Pa) on the physical and photocatalytic property of the powder was investigated. Miao et al. [13] reported the structural and compositional properties of TiO_2 thin films prepared by N_2–H_2 plasma treatment. HRTEM results indicated that the primitive lattice cells of anatase TiO_2 films are distorted after plasma treatment in comparison with that of bulk TiO_2, which confirmed the N doping by N_2–H_2 plasma.

It is shown from the above literatures that N_2 and NH_3 were usually used as nitrogen source to prepare N doped TiO_2 under plasma treatment. However, few literature on the comparison of N_2 and NH_3 plasma treated TiO_2 were reported. In this work, NH_3 plasma, N_2 plasma, and annealing in flowing NH_3 were used to prepare N doped TiO_2, respectively. The structural and optical properties of prepared N doped TiO_2 were compared. The photocatalytic performance was evaluated in the degradation of methylene blue under visible light. The possible mechanism for the photocatalysis was proposed.

* Corresponding author. Tel.: +86 24 23847473.
E-mail address: hushaozheng001@163.com (S. Hu).

0304-3894/$ – see front matter © 2011 Elsevier B.V. All rights reserved.
doi:10.1016/j.jhazmat.2011.09.021

2. Experimental

2.1. Preparation and characterization

The doping of TiO_2 was conducted in a dielectric barrier discharge (DBD) reactor, consisting of a quartz tube and two electrodes. The high voltage electrode was a stainless-steel rod (2.5 mm), which was installed in the axis of the quartz tube and connected to a high voltage supply. The grounding electrode was an aluminum foil, which was wrapped around the quartz tube. For each run, 0.4 g commercial TiO_2 powder (P25) was charged into the quartz tube. At a constant NH_3 flow (40 ml min^{-1}), a high voltage of 9–11 kV was supplied by a plasma generator at an overall power input of 50 V × 0.4 A. The discharge frequency was fixed at 10 kHz, and the discharge was kept for 15 min. After discharge, the reactor was cooled down to room temperature. The obtained TiO_2 sample was denoted as TO–P_{NH_3}. When N_2 was used to replace NH_3 following the same procedure in the preparation of TO–P_{NH_3}, the product is denoted as TO–P_{N_2}. For comparison, P25 was calcined under NH_3 flow (40 ml min^{-1}) for 15 min at 500 °C. The obtained sample was denoted as TO–C_{NH_3}.

XRD patterns of the prepared TiO_2 samples were recorded on a Rigaku D/max-2400 instrument using Cu Kα radiation (λ = 1.54 Å). UV–vis spectroscopy measurement was carried out on a Jasco V-550 spectrophotometer, using $BaSO_4$ as the reference sample. FT-IR spectra were obtained on a Nicolet 20DXB FT-IR spectrometer in the range of 400–2300 cm^{-1}. The zeta-potential of the catalyst was measured at room temperature on Zetasizer Nano S90 (Malvern Instruments). The pH was adjusted by dropwise addition of dilute HCl or NaOH solution. Photoluminescence (PL) spectra were measured at room temperature with a fluorospectrophotometer (FP-6300) using a Xe lamp as excitation source. XPS measurements were conducted on a Thermo Escalab 250 XPS system with Al Kα radiation as the exciting source. The binding energies were calibrated by referencing the C1s peak (284.6 eV) to reduce the sample charge effect.

2.2. Photocatalytic reaction

Methylene blue (MB) was selected as model compound to evaluate the photocatalytic performance of the prepared TiO_2 particles in an aqueous solution under visible light irradiation. 0.1 g TiO_2 powders were dispersed in 100 ml aqueous solution of MB (initial concentration C_0 = 50 ppm, pH 6.8) in an ultrasound generator for 10 min. The suspension was transferred into a self-designed glass reactor, and stirred for 30 min in darkness to achieve the adsorption equilibrium. The concentration of MB at this point was considered as the absorption equilibrium concentration $C_{0'}$. The adsorption capacity of a catalyst to MB was defined by the adsorption amount of MB on the photocatalyst ($C_0 - C_{0'}$). In the photoreaction under visible light irradiation, the suspension was exposed to a 110 W high-pressure sodium lamp with main emission in the range of 400–800 nm, and air was bubbled at 130 ml min^{-1} through the solution. The UV light portion of sodium lamp was filtered by 0.5 M $NaNO_2$ solution [14]. The light intensity is 130 mW cm^{-2}. All runs were conducted at ambient pressure and 30 °C. At given time intervals, 4 ml suspension was taken and immediately centrifuged to separate the liquid samples from the solid catalyst. The concentrations of MB before and after reaction were measured by means of a UV–vis spectrophotometer at a wavelength of 665 nm. It is the linear relationship between absorbance and concentration of liquid sample in the experimental concentration range. Therefore, the percentage of degradation $D\%$ was determined as follows:

$$D\% = \frac{A_0 - A}{A_0} \times 100\% \quad (1)$$

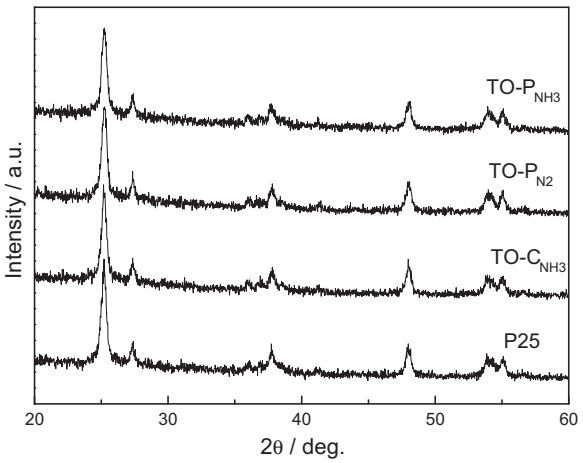

Fig. 1. XRD patterns of P25 and prepared N-doped TiO_2 samples.

where A_0 and A are the absorbances of the liquid sample before and after degradation, respectively.

3. Results and discussion

It is reported that the phase composition and particle size of TiO_2 have significant influence on its photocatalytic activity [2]. The XRD patterns of P25 and prepared N-doped samples (Fig. 1) indicate that all TiO_2 samples were mixtures of anatase and rutile phases. The phase contents and the particle sizes of the samples were calculated by their XRD patterns according to the method of Spurr [15] and Debye–Scherrer equation [16], respectively. The results (Table 1) indicate that there were no remarkable changes in phase composition and particle sizes.

Up to date, the mechanism of the enhancement by N-doping is still controversial. Asahi et al. [3] concluded that the doped N atoms narrowed the band gap of TiO_2 by mixing N 2p and O 2p states, therefore demonstrating the activity. Irie et al. [17] argued that the isolated narrow band located above the valence band is responsible for the visible light response. Lee et al. [18] suggested that substitutional N-doping would narrow the band gap by the coupling of the O 2p and N 2p orbitals, while interstitial N-doping would create an isolated defect state between the conduction band and valence band. Fig. 2 shows the UV–vis spectra of P25 and prepared N-doped TiO_2 samples. Compared with the spectra of P25, obvious red-shifts of the absorption bands were observed for prepared N-doped TiO_2.

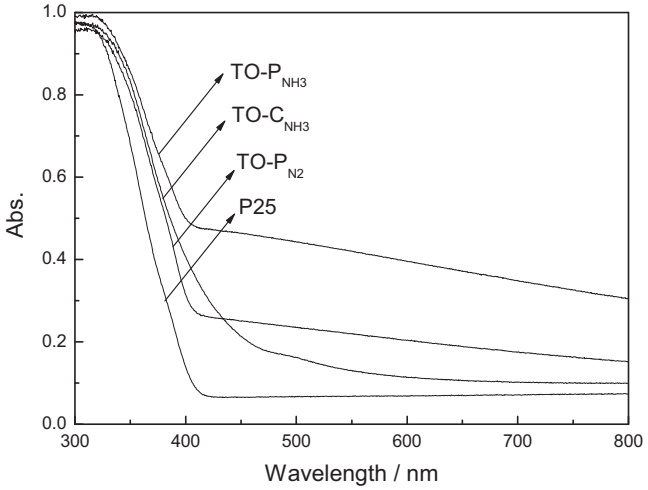

Fig. 2. UV–vis spectra of P25 and prepared N-doped TiO_2 samples.

Table 1
Summary of physical properties of P25 and prepared N-doped TiO_2 samples.

Sample	Size (nm)	X_A (%)[a]	S_{BET} (m^2g^{-1})	Pore volume (cm^3g^{-1})	Central pore size (nm)	E_g (eV)	N_{fresh} (at.%)[b]	N_{used} (at.%)[c]
P25	28.2	74.6	43	0.07	3.6	3.10	0	0
TO–P_{N_2}	28.5	74.7	40	0.06	3.2	2.92	1.32	0.76
TO–C_{NH_3}	29.3	74.4	36	0.05	3.1	2.75	1.64	1.17
TO–P_{NH_3}	28.1	75.1	41	0.06	3.4	2.67	1.95	1.91

[a] X_A represents the phase composition of anatase.
[b] N_{fresh} represents the lattice-nitrogen content before photocatalytic reaction
[c] N_{used} represents the lattice-nitrogen content after photocatalytic reaction.

The band gap energies of TiO_2 samples which calculated according to the method of Oregan and Gratzel [19] (Table 1) indicate that the prepared N-doped TiO_2 samples exhibited much narrowed band gap energies. According to the previous result [3,18], this indicated that substitutional N-doping existed in the prepared N-doped TiO_2 samples. It is shown that the band gap energy decreased in the order: TO–P_{N_2} > TO–C_{NH_3} > TO–P_{NH_3}, which is probably due to the different doping N content in prepared N-doped TiO_2 samples. Xu et al. [20] prepared N doped TiO_2 by pulsed laser deposition and suggested that more absorption edge red-shift indicated higher nitrogen concentration. Besides, the distinct differences in visible light absorption are observed between calcination and plasma treated samples. In the spectrum of TO–C_{NH_3}, the obvious absorption in 400–550 nm is observed, which is a typical absorption region for N doped TiO_2 materials. This typical absorption is due to the electronic transition from the isolated N 2p level, which is formed by incorporation of nitrogen atoms into the TiO_2 lattice, to the conduction band [21]. However, the spectra of plasma treated samples are obvious different. The broad absorptions in the whole visible light region are observed in the spectra of TO–P_{N_2} and TO–P_{NH_3}. Huang et al. [22] prepared the visible light responsive TiO_2 by nitrogen-plasma surface treatment, and found the similar broad absorption in visible light region. Abe et al. [12] prepared N doped TiO_2 by NH_3/Ar plasma, and suggested that such broad absorption is attributed to the presence of Ti^{3+}, which might be formed by plasma treatment. It is noted that TO–P_{NH_3} showed much stronger broad absorption in visible light region than TO–P_{N_2}. This is probably due to that NH_3 plasma consists of not only various active nitrogen species but excited hydrogen, leading to Ti^{4+} reduced easily, thus more Ti^{3+} were formed. Therefore, according to the conclusion of Lee et al. [18], it is proposed that substitutional and interstitial N-doping existed simultaneously in TO–C_{NH_3} which caused the band gap narrowing and remarkable absorption in 400–550 nm, whereas only substitutional N-doping existed in TO–P_{N_2} and TO–P_{NH_3}. The broad absorptions of TO–P_{N_2} and TO–P_{NH_3} in the whole visible light region were due to the presence of Ti^{3+} caused by the N-doping.

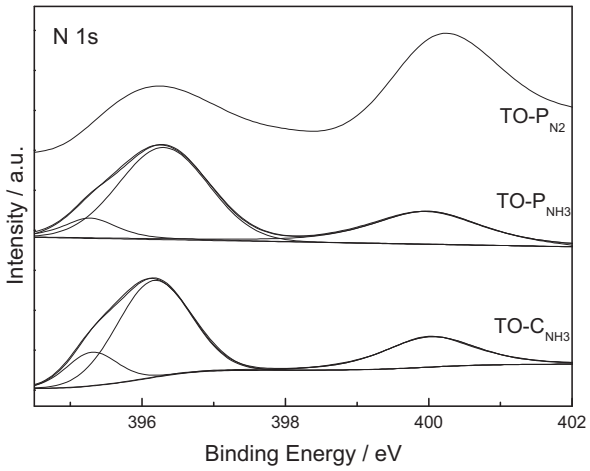

Fig. 3. XP spectra of prepared N-doped TiO_2 samples in the region of N1s.

XPS is an effective surface test technique to characterize elemental composition and chemical states. According to the previous literatures [10,11], the peaks around 396 and 400 eV are attributed to the formation of lattice-nitrogen and other surface N species such as N–N and N–O bond. The XP spectra in the region of N1s (Fig. 3) indicated that most N species in prepared TiO_2 using NH_3 as nitrogen source existed in lattice-nitrogen, whereas other surface N species such as N–N and N–O bond were dominant in TO–P_{N_2} which using N_2 as nitrogen source. The lattice-nitrogen content calculated by XPS data were shown in Table 1. The N_{fresh} content decreased in the order: TO–P_{NH_3} > TO–C_{NH_3} > TO–P_{N_2}, which indicated that NH_3 plasma treatment is more effective than another two methods

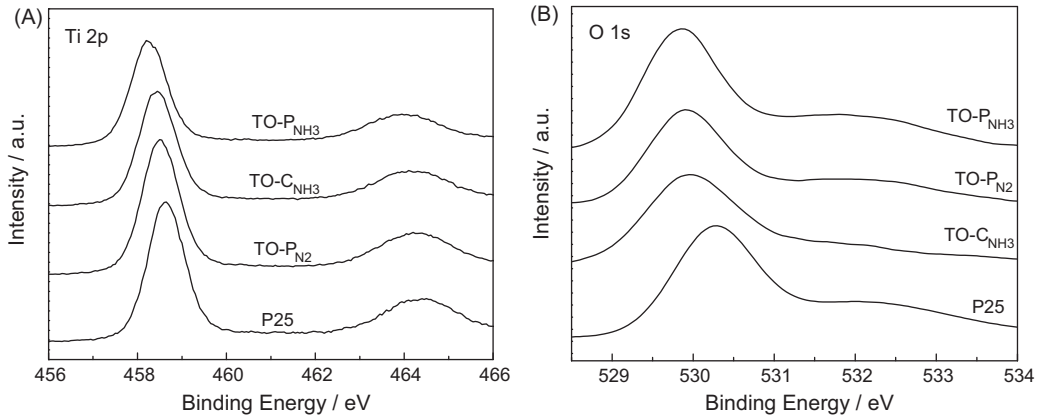

Fig. 4. XP spectra of P25 and prepared N-doped TiO_2 samples in the region of Ti 2p (A) and O1s (B).

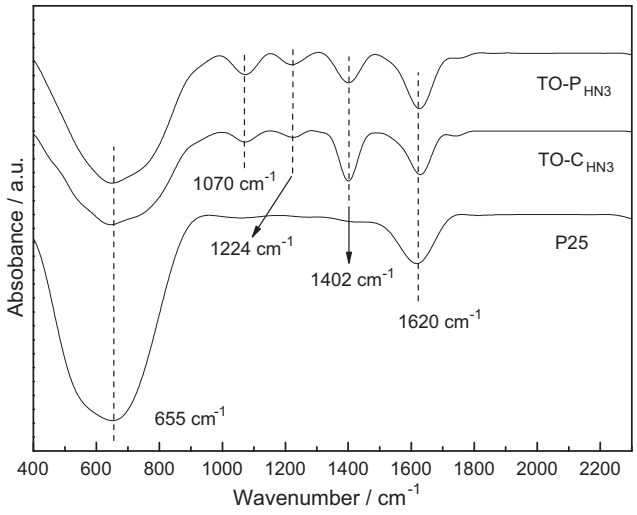

Fig. 5. FT-IR spectra of P25, TO–C_{NH_3} and TO–P_{NH_3}.

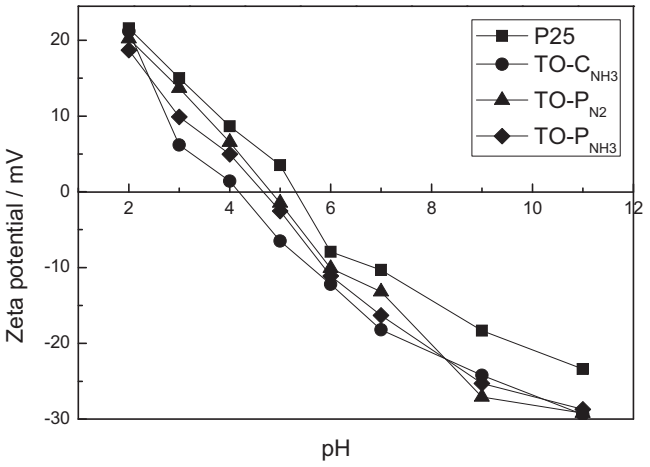

Fig. 6. Plots of the zeta-potential as a function of pH for P25 and prepared N-doped TiO_2 suspensions in the presence of NaCl (10^{-3} M).

to form lattice-nitrogen. This is probably due to that NH_3 plasma consists of various nitriding species, leading to the formation of lattice-nitrogen easier [23]. Besides, trace N species, which located at 395.3 eV were present in TO–P_{NH_3} and TO–C_{NH_3}. Li et al. [24] prepared N doped TiO_2 in NH_3/ethanol fluid under supercritical condition, and suggested that the N species with binding energy at 395.3 eV was attributed to the surface adsorbed NH_3 molecules. In this investigation, the N species located at 395.3 eV only existed in TO–P_{NH_3} and TO–C_{NH_3}, which prepared using NH_3 as nitrogen source. This confirmed the result of Li et al. Furthermore, the peak intensity of TO–C_{NH_3} at 395.3 eV was obvious higher than that of TO–P_{NH_3}, indicating more NH_3 molecules adsorbed on TO–C_{NH_3} surface.

Fig. 4 shows the XP spectra of P25 and prepared N-doped TiO_2 samples in the region of Ti 2p and O1s. Compared with the spectra of P25, obvious shifts to lower binding energies were observed for N-doped TiO_2 samples in the Ti 2p region (458.4 eV) as well as the O1s region (529.7 eV). This is probably attributed to the change of chemical environment after N doping [24]. It is known that the binding energy of the element is influenced by its electron density. A decrease in binding energy implies an increase of the electron density. The electrons of N atoms may be partially transferred from N to Ti and O, due to the higher electronegativity of oxygen, leading to increased electron densities on both Ti and O. The peaks around 530 and 532 eV in the O1s region are attributed to crystal lattice oxygen (Ti–O) and surface hydroxyl group (O–H) of TiO_2. The ratio of these two peak areas (S_{O-H}/S_{Ti-O}) represents the abundance of surface hydroxyl groups. The calculated results indicated that S_{O-H}/S_{Ti-O} ratio for TO–C_{NH_3} was 0.06, much lower than that of P25 (0.14). Whereas, S_{O-H}/S_{Ti-O} ratios for TO–P_{N_2} and TO–P_{NH_3} were 0.13 and 0.11, which were slight lower than P25. This indicated the content of surface hydroxyl groups decreased more drastically after the calcination procedure under NH_3 flow compared with plasma treatment. Those surface hydroxyl groups are known to play an important role in photocatalysis. They react with photogenerated holes, producing active hydroxyl radicals, which are responsible for the photo-degradation [25].

The FT-IR spectra of P25 and TO–P_{NH_3} were shown in Fig. 5. The absorption peak at 1620 cm^{-1} is attributed to bending vibration of hydroxyl group. The band at around 655 cm^{-1} belongs to O–Ti–O structure of TiO_2. There are three bands at 1402, 1224, and 1070 cm^{-1} which were observed in the spectra of TO–C_{NH_3} and TO–P_{NH_3}, but not in that of P25. The band at 1402 cm^{-1} is attributed to the surface adsorbed NH_3 species on Brönsted acid sites (–OH) [26]. It is known that NH_3 can adsorb on Brönsted acid sites (–OH) located at 1400 cm^{-1} and Lewis acid sites (Ti^{4+}) located at 1225 and 1190 cm^{-1} [26,27]. However, in Fig. 5, no NH_3 adsorbed on the Lewis acid sites was observed. There are many previous literatures, which report the FT-IR results of NH_3 adsorbed on TiO_2 materials. Some of them reported that NH_3 adsorbed on both Brönsted acid and Lewis acid sites [26,27]. Other results showed that only adsorption on Brönsted acid sites was obtained which is consistent with the result of Fig. 5 [24,28]. Therefore, it is proposed that the preparation methods and conditions probably affect the adsorption state, leading to the adsorption site different from different literatures. It is known that the TiO_2 surface is hydrophilic. In this investigation, TiO_2 materials were treated under calcination and plasma condition only for 15 min, leading to most of the H_2O adsorbed on Ti^{4+} still existed on TiO_2 surface. It is reported that when Ti^{4+} sites are saturated by hydroxyl groups, NH_3 will adsorb mainly on Brönsted acid sites by the formation of an N···HO bond [29]. Therefore, only adsorption on Brönsted acid sites was obtained. In Fig. 5, the peaks at 1224 and 1070 cm^{-1} could be attributed to the nitrogen atoms embedded in the TiO_2 network, which is consistent with XPS result [28]. These results confirmed the formation of doping N species in the TiO_2 lattice.

Fig. 6 shows the plots of the zeta-potential as a function of pH for P25 and prepared N-doped TiO_2 suspensions in the presence of NaCl (10^{-3} M). It is known that the point of zero charge (PZC) of TiO_2 is around 3–6, indicating the surface of TiO_2 particles is positively charged. Compared with P25, the distinct shifts to lower value of the PZC were observed for all the N doped TiO_2, indicating the positive charge on TiO_2 surface decreased. The PZC value decreased in the order: P25 > TO–P_{N_2} > TO–P_{NH_3} > TO–C_{NH_3}. It is possible that the lone electron pair of doping N counteract a few of positive charge. Besides, NH_3 readily adsorbed on the catalyst surface during the nitridation process, due to the numerous acidic hydroxyl groups on the TiO_2 surface. The presence of these surface-adsorbed NH_3 decreased the number of acidic hydroxyl groups, resulting in lower PZC value of TO–P_{NH_3} and TO–C_{NH_3}. Furthermore, plasma treatment caused the NH_3 decomposition more drastically, leading to less NH_3 adsorbed on TO–P_{NH_3} surface compared with TO–C_{NH_3}. Therefore, the PZC value of TO–P_{NH_3} is higher than TO–C_{NH_3}.

The adsorption of MB on TiO_2-based catalysts was measured by the equilibrium adsorption capacity. The adsorption capacities of all the N doped TiO_2 samples were lower than that of P25 (Fig. 7). The BET specific surface area (S_{BET}), pore volume, and central pore size are listed in Table 1. Compared with P25, the S_{BET}, pore volume, and central pore size of prepared samples decreased.

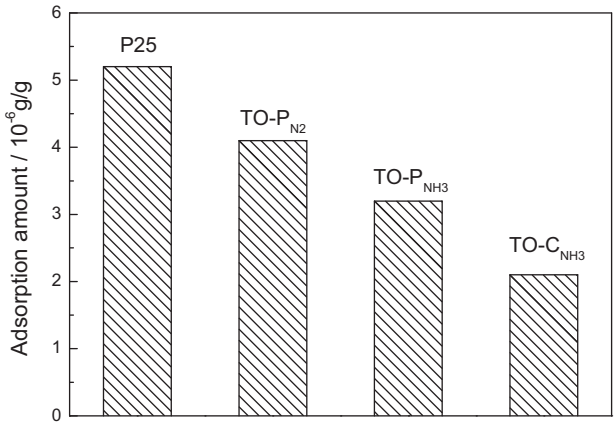

Fig. 7. Adsorption capacity of MB on P25 and N-doped TiO_2 samples.

This probably caused the decreased equilibrium adsorption capacity shown in Fig. 7. Besides, it is possibly that such decreased adsorption of MB is attributed to the coverage of TiO_2 surface by excess surface N species. It is noted that the equilibrium adsorption capacity decreased in the order: P25 > TO–P_{N_2} > TO–P_{NH_3} > TO–C_{NH_3}, which is completely consistent with the order of surface hydroxyl groups content. This indicated that the content of surface hydroxyl groups influenced significantly on the equilibrium adsorption capacity. It is shown that equilibrium adsorption capacities of TO–P_{NH_3} and TO–C_{NH_3} were lower than TO–P_{N_2}, which using N_2 as nitrogen source. Besides the lower surface hydroxyl groups content than that of TO–P_{N_2}, large numbers of NH_3 molecules adsorbed on hydroxyl groups of TO–P_{NH_3} and TO–C_{NH_3}, caused the reduced surface sites for adsorbing MB, leading to lower equilibrium adsorption capacity than TO–P_{N_2}.

The photocatalytic performances under visible light shown in Fig. 8 indicate that prepared N-doped TiO_2 samples exhibited much higher activities than that of P25. Since no obvious change were observed in phase compositions and particle sizes between P25 and prepared N-doped TiO_2 samples, the enhanced photocatalytic activity must result from the doping of nitrogen in TiO_2, which gave rise to the narrowed band gap and thus to the enhanced absorption in the visible region. Moreover, it is shown that the photocatalytic activity increased in the order: TO–P_{N_2} > TO–C_{NH_3} > TO–P_{NH_3}, which is in agreement with the order of lattice-nitrogen content (N_{fresh}). This proved that the lattice-nitrogen significantly

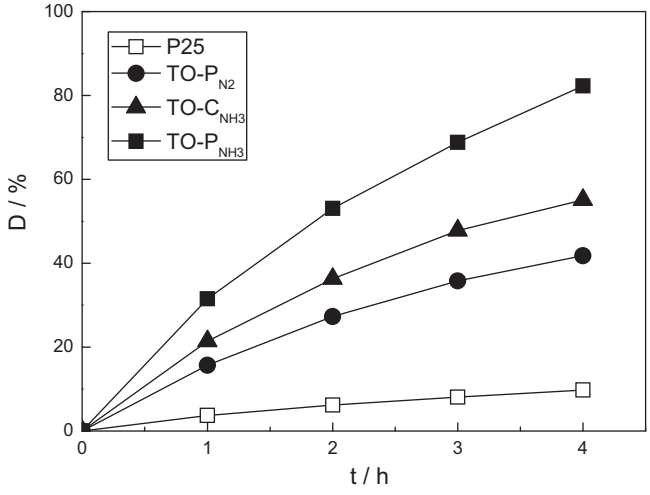

Fig. 8. Photocatalytic performances of P25 and prepared N-doped TiO_2 samples in the degradation MB under visible light irradiation.

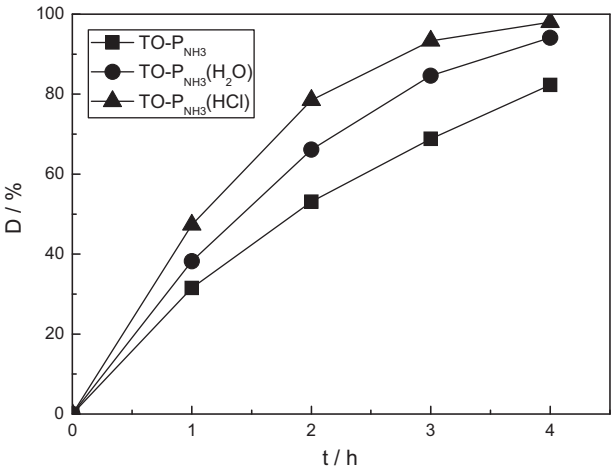

Fig. 9. Photocatalytic performances of TO–P_{NH_3}, TO–$P_{NH_3}(H_2O)$, and TO–P_{NH_3}(HCl) in the degradation MB under visible light irradiation.

influenced the visible light activity, which is consistent with the earlier results of Yamada [10]. On the other hand, the stronger absorption in visible light region of TO–P_{NH_3} caused the visible light utilization more effectively, thus leading to the much higher activity than that of TO–P_{N_2} and TO–C_{NH_3}. N_{used} is calculated and shown in Table 1. Obviously, N_{used} of TO–C_{NH_3} and TO–P_{N_2} are much lower than that of N_{fresh}, whereas lattice-nitrogen of TO–P_{NH_3} is relatively stable. It is reported that the lattice-nitrogen was oxidated by photogenerated holes during the degradation reaction, leading to the decrease of lattice-nitrogen content [30]. Therefore, it is deduced that the oxidation of lattice-nitrogen of TO–P_{NH_3} is more difficult than that of another two samples. This difference in lattice-nitrogen stability is probably due to the different preparation method among three samples. Besides, Chen et al. [30] prepared N doped TiO_2 by heating TiO_2 powders in NH_3 flow and found that the presence of surface-adsorbed NH_3 decreased the number of surface sites accessible for reactants, resulting in low photocatalytic activity. In this investigation, compared with TO–P_{NH_3}, more NH_3 adsorbed on TO–C_{NH_3} surface, thus leading to the lower adsorption capacity and photocatalytic activity of TO–C_{NH_3}.

To confirm the detrimental effect of NH_3, Chen et al. [30] washed the prepared N doped TiO_2 with pure water for several times to remove adsorbed NH_3. The photocatalytic activity of obtained sample was improved after washing, but still much lower than that of postcalcination sample (NT400). This is probably due to that NH_3 was not removed completely by washing with pure water. In this investigation, TO–P_{NH_3} was washed with HCl (0.1 M) to remove the adsorbed NH_3, and then cleaned with deionized water. The obtained sample was denoted as TO–P_{NH_3}(HCl). For comparison, TO–$P_{NH_3}(H_2O)$ was obtained by washing TO–P_{NH_3} with deionized water directly. The FT-IR results (not shown) indicated that adsorbed NH_3 were removed completely after HCl washing, whereas residual NH_3 still existed on TO–$P_{NH_3}(H_2O)$ surface. The photocatalytic performances (Fig. 9) show that the activity increased in the order: TO–P_{NH_3} < TO–$P_{NH_3}(H_2O)$ < TO–P_{NH_3}(HCl), which confirmed NH_3 detrimental effect on photocatalytic activity.

When TO–P_{N_2} and TO–C_{NH_3} were used to replace TO–P_{NH_3} following the same procedure as in the preparation of TO–P_{NH_3}(HCl), the product were denoted as TO–P_{N_2}(HCl) and TO–C_{NH_3}(HCl), respectively. The photocatalytic performances of TO–P_{N_2}(HCl), TO–C_{NH_3}(HCl), and TO–P_{NH_3}(HCl) were investigated in three cycles to check the photocatalytic stability (Fig. 10). It is shown that the activity of TO–P_{NH_3}(HCl) decreased slightly in 1st reuse and kept stable in the next two cycles. However, for TO–P_{N_2}(HCl) and

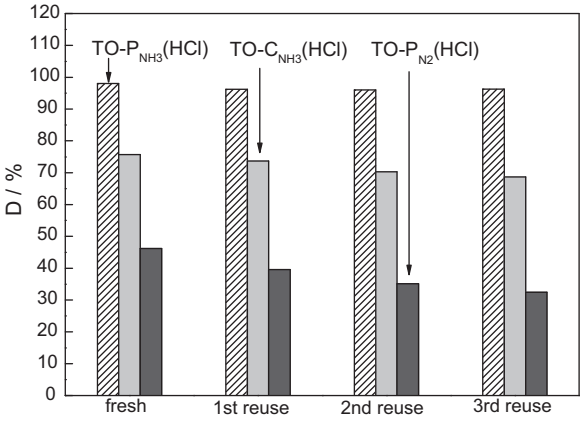

Fig. 10. Photocatalytic stability of prepared N-doped TiO_2 samples in the degradation of MB.

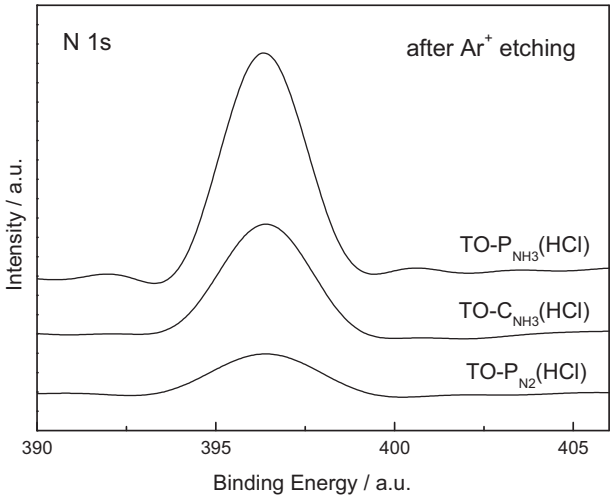

Fig. 11. XP spectra of TO–P_{N_2}(HCl), TO–C_{NH_3}(HCl), and TO–P_{NH_3}(HCl) in the region of N1s after Ar^+ ion etching.

TO–C_{NH_3}(HCl), the activities decreased gradually, from 41.8% and 55.1% for fresh catalyst to 30.9% and 49.6% for 3rd reused catalyst. This hinted that the photocatalytic stability of TO–P_{NH_3}(HCl) was much better than TO–P_{N_2}(HCl) and TO–C_{NH_3}(HCl). It is proposed that this difference in photocatalytic stability is attributed to the different lattice-nitrogen stability among the three samples. Therefore, the lattice-nitrogen contents of fresh and reused TO–P_{N_2}(HCl), TO–C_{NH_3}(HCl), and TO–P_{NH_3}(HCl) were calculated according to the relevant XPS data (Table 2). The lattice-nitrogen contents of TO–P_{N_2}(HCl) and TO–C_{NH_3}(HCl) decreased gradually from 1.28 at.% and 1.62 at.% to 0.46 at.% and 1.04 at.% after three cycles which confirmed that the lattice-nitrogen significantly influenced the visible light activity. However, lattice-nitrogen content of TO–P_{NH_3}(HCl) decreased slightly from 1.94 at.% to 1.78 at.% for the 1st reuse, and then kept stable in the next two cycles. This indicated that the lattice-nitrogen atoms in TO–P_{NH_3}(HCl) remained relatively stable.

As mentioned above, N_{used} of TO–C_{NH_3} and TO–P_{N_2} are much lower than that of N_{fresh}, whereas lattice-nitrogen of TO–P_{NH_3} is stable (Table 1). This difference in lattice-nitrogen stability is probably due to the different preparation method among three samples. In order to elucidate why the photocatalytic stability is different among the samples, the XP spectra of fresh TO–P_{N_2}(HCl), TO–C_{NH_3}(HCl), and TO–P_{NH_3}(HCl) in N1s region after Ar^+ ion etching were measured and shown in Fig. 11. Apparently, the surface adsorbed NH_3 species located at 395.3 eV and N–N (N–O) species located at 400 eV were removed after Ar^+ ion etching to get rid of the surface layer. Only one peak around 396 eV, which attributed to lattice-nitrogen was observed for all the three samples. The calculation according to the relevant XPS data revealed that the lattice-nitrogen content of TO–P_{N_2}(HCl), TO–C_{NH_3}(HCl), and TO–P_{NH_3}(HCl) were 0.32, 0.74, and 1.58 at.%, respectively. Compared with the data of fresh catalyst in Table 2, more than 50% and 75% lattice-nitrogen in TO–C_{NH_3}(HCl) and TO–P_{N_2}(HCl) was eliminated after Ar^+ ion etching. This indicated that a great number of N atoms doped only into the surface layer of TO–C_{NH_3}(HCl) and TO–P_{N_2}(HCl), which were oxidated easily by photogenerated holes during the degradation reaction, leading to the decrease of lattice-nitrogen content. Therefore, TO–P_{N_2} and TO–C_{NH_3} exhibited the poor photocatalytic stability. On the contrary, compared with the data of fresh TO–P_{NH_3}(HCl) in Table 2, less than 20% lattice-nitrogen of TO–P_{NH_3}(HCl) was removed after Ar^+ ion etching. This is probably due to that the excited hydrogen species produced by NH_3 plasma made the N atoms doped into crystal lattice of deeper layer, thus caused it oxidated difficulty by photogenerated holes. Therefore, the photocatalytic stability of TO–P_{NH_3}(HCl) was much higher than that of TO–P_{N_2} and TO–C_{NH_3}.

Table 2
Lattice-nitrogen content of fresh and reused TO–P_{NH_3}(HCl), TO–C_{NH_3}(HCl), and TO–P_{N_2}(HCl) determined by XPS data.

Sample	Fresh catalyst (at.%)	1st recycle (at.%)	2nd recycle (at.%)	3rd recycle (at.%)
TO–P_{NH_3}(HCl)	1.94	1.78	1.78	1.75
TO–C_{NH_3}(HCl)	1.62	1.31	1.22	1.04
TO–P_{N_2}(HCl)	1.28	1.02	0.75	0.46

Table 3
Comparison of lattice-nitrogen stability of N-doped TiO_2 samples before and after HCl solution washing.

Sample	Fresh catalyst (at.%)	1st reuse (at.%)	Retention rate[a]
TO–P_{NH_3}(HCl)	1.94	1.78	0.92
TO–C_{NH_3}(HCl)	1.62	1.31	0.81
TO–P_{N_2}(HCl)	1.28	1.02	0.80
TO–P_{NH_3}	1.95	1.91	0.98
TO–C_{NH_3}	1.64	1.17	0.71
TO–P_{N_2}	1.32	0.76	0.58

[a] Retention rate is equal to the ratio of lattice-nitrogen content in 1st reused catalyst to that of fresh catalyst.

The retention rate of lattice-nitrogen, which represents the lattice-nitrogen stability is calculated and shown in Table 3. Compared with the sample before HCl washing, more than 10% and 20% enhancement of retention rate are observed in TO–C_{NH_3}(HCl) and TO–P_{N_2}(HCl), whereas only slight decrease of retention rate is shown in TO–P_{NH_3}(HCl). This indicated the lattice-nitrogen stability of N-doped TiO_2 samples improved after HCl solution washing. This is probably due to that the surface N species absorbed on Brönsted acid sites (–OH) were removed by HCl solution, leading to more surface hydroxy groups are available to trap the photogenerated holes, thus restrain the oxidation of lattice-nitrogen by photo-generated holes.

4. Conclusion

NH_3 plasma, N_2 plasma, and annealing in flowing NH_3 were used to prepare N doped TiO_2 respectively to investigate the influence of preparation method, nitrogen source, and post-treatment on the photocatalytic activity and stability. The photocatalytic activity increased in the order: TO–P_{N_2} < TO–C_{NH_3} < TO–P_{NH_3}, indicating NH_3 plasma is most effective among the three

methods. The lattice-nitrogen significantly influenced the visible light activity. NH_3 which adsorbed on catalyst surface led to the low adsorption capacity for reactant MB, thus decreased photocatalytic activity. After removal NH_3 by HCl washing, the obtained catalysts exhibited much higher activities under visible light, which confirmed the detrimental effect of NH_3. The photocatalytic stability of N doped TiO_2 prepared by NH_3 plasma was much higher than that of samples prepared by other nitridation procedures. This is proposed that the excited hydrogen species produced by NH_3 plasma made the N atoms doped into crystal lattice of deeper layer, which caused it oxidated more difficult by photogenerated holes than other catalysts, thus leading to the stable lattice-nitrogen. Besides, the lattice-nitrogen stability of N-doped TiO_2 samples improved after HCl solution washing. This is probably due to that the surface N species absorbed on Brönsted acid sites (–OH) were removed by HCl solution, leading to more surface hydroxy group are available to trap the photo-generated holes, thus restrain the oxidation of lattice-nitrogen. This stable lattice-nitrogen during the degradation reaction caused the high photocatalytic stability.

Acknowledgments

This work was supported by National Natural Science Foundation of China (no. 41071317, 30972418), National Key Technology R & D Programme of China (no. 2007BAC16B07), the Natural Science Foundation of Liaoning Province (no. 20092080). The authors would like to thank Prof. Anjie Wang, Dalian University of Technology, for the contribution to the manuscript.

References

[1] A. Fujishima, T.N. Rao, D.A. Tryk, Titanium dioxide photocatalysis, J. Photochem. Photobiol. C 1 (2000) 1–21.
[2] M.R. Hoffmann, S.T. Martin, W. Choi, D.W. Bahnemann, Environmental applications of semiconductor photocatalysis, Chem. Rev. 95 (1995) 69–96.
[3] R. Asahi, T. Morikawa, T. Ohwaki, A. Aoki, Y. Taga, Visible-light photocatalysis in nitrogen-doped titanium oxides, Science 293 (2001) 269–271.
[4] T. Lindgren, J.M. Mwabora, E. Avendano, J. Jonsson, A. Hoel, C.G. Granqvist, S.E. Lindquist, Photoelectrochemical and optical properties of nitrogen doped titanium dioxide films prepared by reactive DC magnetron sputtering, J. Phys. Chem. B 107 (2003) 5709–5716.
[5] M. Qiao, S.S. Wu, Q. Chen, J. Shen, Novel triethanolamine assisted sol–gel synthesis of N-doped TiO_2 hollow spheres, Mater. Lett. 12 (2010) 1398–1400.
[6] H. Shen, L. Mi, P. Xu, W.D. Shen, P.N. Wang, Visible-light photocatalysis of nitrogen-doped TiO_2 nanoparticulate films prepared by low-energy ion implantation, Appl. Surf. Sci. 17 (2007) 7024–7028.
[7] L. Zhao, Q. Jiang, J.S. Lian, Visible-light photocatalytic activity of nitrogen-doped TiO_2 thin film prepared by pulsed laser deposition, Appl. Surf. Sci. 15 (2008) 4620–4625.
[8] S.Z. Hu, A.J. Wang, X. Li, H. Löwe, Hydrothermal synthesis of well-dispersed ultrafine N-doped TiO_2 nanoparticles with enhanced photocatalytic activity under visible light, J. Phys. Chem. Solid 71 (2010) 156–162.
[9] K. Yamada, H. Nakamura, S. Matsushima, H. Yamane, T. Haishi, K. Ohira, K. Kumada, Preparation of N-doped TiO_2 particles by plasma surface modification, C. R. Chimie 9 (2006) 788–793.
[10] K. Yamada, H. Yamane, S. Matsushima, H. Nakamura, K. Ohira, M. Kouya, K. Kumada, Effect of thermal treatment on photocatalytic activity of N-doped TiO_2 particles under visible light, Thin Solid Films 516 (2008) 7482–7487.
[11] K. Yamada, H. Yamane, S. Matsushima, H. Nakamura, T. Sonoda, S. Miura, K. Kumada, Photocatalytic activity of TiO_2 thin films doped with nitrogen using a cathodic magnetron plasmatreatment, Thin Solid Films 516 (2008) 7560–7564.
[12] H. Abe, T. Kimitani, M. Naito, Influence of NH_3/Ar plasma irradiation on physical and photocatalytic properties of TiO_2 nanopowder, J. Photochem. Photobiol. A 183 (2006) 171–175.
[13] L. Miao, S. Tanemura, H. Watanabe, S. Toh, K. Kaneko, Structural and compositional characterization of N_2–H_2 plasma surface-treated TiO_2 thin films, Appl. Surf. Sci. 244 (2005) 412–417.
[14] F.B. Li, X.Z. Li, M.F. Hou, K.W. Cheah, W.C.H. Choy, Enhanced photocatalytic activity of Ce^{3+}–TiO_2 for 2-mercaptobenzothiazole degradation in aqueous suspension for odour control, Appl. Catal. A 285 (2005) 181–189.
[15] R.A. Spurr, H. Myers, Quantitative analysis of anatase–rutile mixtures with an X-ray diffractometer, Anal. Chem. 29 (1957) 760–762.
[16] J. Lin, Y. Lin, P. Liu, M.J. Meziani, L.F. Allard, Y.P. Sun, Hot-fluid annealing for crystalline titanium dioxide nanoparticles in stable suspension, J. Am. Chem. Soc. 124 (2002) 11514–11518.
[17] H. Irie, Y. Watanaba, K. Hashimoto, Nitrogen-concentration dependence on photocatalytic activity of $TiO_{2-x}N_x$ powders, J. Phys. Chem. B 107 (2003) 5483–5486.
[18] S. Lee, I. Cho, D.K. Lee, D.W. Kim, T.H. Noh, C.H. Kwak, S. Park, K.S. Hong, J. Lee, H.S. Jung, Influence of nitrogen chemical states on photocatalytic activities of nitrogen-doped TiO_2 nanoparticles under visible light, J. Photochem. Photobiol. A 213 (2010) 129–135.
[19] B. Oregan, M. Gratzel, A low-cost, high-efficiency solar-cell based on dye-sensitized colloidal TiO_2 films, Nature 353 (1991) 737–740.
[20] P. Xu, L. Mi, P.N. Wang, Improved optical response for N-doped anatase TiO_2 films prepared by pulsed laser deposition in $N_2/NH_3/O_2$ mixture, J. Cryst. Growth 289 (2006) 433–439.
[21] H. Ozaki, N. Fujimoto, S. Iwamoto, M. Inoue, Photocatalytic activities of NH_3-treated titanias modified with other elements, Appl. Catal. B 70 (2007) 431–436.
[22] C.M. Huang, L.C. Chen, K.W. Cheng, G.T. Pan, Effect of nitrogen-plasma surface treatment to the enhancement of TiO_2 photocatalytic activity under visible light irradiation, J. Mol. Catal. A 261 (2007) 218–224.
[23] S. Luan, G.W. Neudeck, Effect of NH_3 plasma treatment of gate nitride on the performance of amorphous silicon thin film transistors, J. Appl. Phys. 68 (1990) 3445–3450.
[24] H.X. Li, J.X. Li, Y.N. Huo, Highly active TiO_2N photocatalysts prepared by treating TiO_2 precursors in NH_3/ethanol fluid under supercritical conditions, J. Phys. Chem. B 110 (2006) 1559–1565.
[25] S.Z. Hu, A.J. Wang, X. Li, Y. Wang, H. Löwe, Hydrothermal synthesis of ionic liquid [Bmim]OH modified TiO_2 nanoparticles with enhanced photocatalytic activity under visible light, Chem. Asian J. 5 (2010) 1171–1177.
[26] J.M.G. Amores, V.S. Escribano, G. Ramis, G. Busca, An FT-IR study of ammonia adsorption and oxidation over anatase-supported metal oxides, Appl. Catal. B 13 (1997) 45–58.
[27] D.A. Peña, B.S. Uphade, P.G. Smirniotis, TiO_2-supported metal oxide catalysts for low-temperature selective catalytic reduction of NO with NH_3 I. Evaluation and characterization of first row transition metals, J. Catal. 221 (2004) 421–431.
[28] J.H. Xu, W.L. Dai, J.X. Li, Y. Cao, H.X. Li, H.Y. He, K.N. Fan, Simple fabrication of thermally stable apertured N-doped TiO_2 microtubes as a highly efficient photocatalyst under visible light irradiation, Catal. Commun. 9 (2008) 146–152.
[29] A. Markovits, J. Ahdjoudj, C. Minot, A theoretical analysis of NH_3 adsorption on TiO_2, Surf. Sci. 365 (1996) 649–661.
[30] X.F. Chen, X.C. Wang, Y.D. Hou, J.H. Huang, L. Wu, X.Z. Fu, The effect of postnitridation annealing on the surface property and photocatalytic performance of N-doped TiO_2 under visible light irradiation, J. Catal. 255 (2008) 59–67.